

Probing vibrational energy relaxation in proteins using normal modes

Hiroshi FUJISAKI* Lintao BU† and John E. STRAUB‡

Department of Chemistry, Boston University, 590 Commonwealth Ave.,
Boston, Massachusetts, 02215, USA

February 9, 2020

Abstract

Vibrational energy relaxation (VER) of a selected mode in cytochrome c (hemeprotein) in vacuum is studied using two theoretical approaches: One is the equilibrium simulation approach with quantum correction factors, and the other is the reduced model approach which describes the protein as an ensemble of normal modes coupled with nonlinear coupling elements. Both methods result in estimates of VER time (sub ps) for a CD stretching mode in the protein at room temperature, that are in accord with the experimental data of Romesberg's group. The applicability of the two methods is examined through a discussion of the validity of Fermi's golden rule on which the two methods are based.

1 Introduction

The harmonic (or normal mode) approximation has been a powerful tool for the analysis of few and many-body systems where the essential dynamics of the system consists of small oscillations about a well-defined mechanically stable structure. The concept of normal modes (NMs) is appealing in science because it provides a simple view for complex systems like solids and proteins. Though it had been believed that NMs may be too simplistic to analyze the dynamics of proteins, that is by no means always true: the experimental data of neutron scattering for proteins (B factor) indicate that the fluctuations for each residue are well represented by a simplified model using NMs [1]. It was also shown that such a large-amplitude motion as the hinge-bending motion in a protein is well described by a NM [2]. Importantly, NMs have been used to refine the x-ray structures of proteins [3]. Recently, large proteins or even protein complexes can be analyzed by using NMs [4, 5, 6].

In this chapter, we are concerned with vibrational energy relaxation (VER) in a protein. This subject is related to our understanding of the functionality of proteins: At the most fundamental level, we must understand the energy flow (pathway) of an injected energy, that is channeled to do useful work. In this chapter, we mainly focus on the VER rate (or time) that characterizes the energy flow. Due to the advance of laser technology, time-resolved spectroscopy can detect such energy flow phenomena experimentally [7]. To interpret experimental data, and to suggest new experiments, theoretical approaches and simulations are essential as they can provide a detailed view of VER. However, VER in large molecules itself is still a challenging problem in molecular science [8]. This is because VER is a typical many-body

*fujisaki@bu.edu

†bult@bu.edu

‡straub@bu.edu

compare the validity of the existing theoretical methods.

We here employ two different methods to estimate the VER rate in a protein, cytochrome c (see the next section for details). One is the classical equilibrium simulation method [10] with quantum correction factors [11, 12]. The second is the reduced model approach [13], which has been recently employed by Leitner's group [14, 15]. The latter approach is based on NM concepts, which describes VER as energy transfers between NMs mediated by nonlinear resonance [16]. We conclude with a discussion of the validity and applicability of such approaches.

2 Cytochrome c

Cytochrome c (cyt c) is one of the most thoroughly physicochemically characterized metalloproteins [17, 18]. It consists of a single polypeptide chain of 104 amino acid residues and is organized into a series of five α -helices and six β -turns. The heme active site in cyt c consists of a 6-coordinate low-spin iron that binds His18 and Met80 as the axial ligands. In addition, two cysteines (Cys14 and Cys17) are covalently bonded through thioether bridges to the heme (see Fig. 1). Crystal structures of cyt c show that the heme group, which is located in a groove and almost completely buried inside the protein, is non-planar and somewhat distorted into a saddle-shape geometry. The reduced protein, ferrocytocytocrome c (ferrocyt c), is relatively compact and very stable, due to the fact that the heme group is neutral.

The vibrational mode we have chosen for study is the isotopically labeled C-D stretch in the terminal methyl group of the residue Met80, which is covalently bonded to Fe in heme (see Fig. 1). Our simulation model approximates the protein synthesized by Romesberg's group [19] though their protein contains three deuteriums in Met80 (Met80-3D). The C-H and C-D stretching bands are located near 3000 cm^{-1} and 2200 cm^{-1} , respectively. In contrast with the modeling of photolyzed CO in myoglobin [10], essentially a diatomic molecule in a protein "solvent," we are interested in the relaxation of a selected vibrational mode of a protein. As a result, the modeling is more challenging: There is no clean separation between the system and bath modes because the CD bond is strongly connected to the environment.

In Fig. 2, we show the density of states (DOS) for cyt c in vacuum and in water at 300K. These are the instantaneous normal mode (INM) spectra, so they contain some negative (actually imaginary) components. The basic structure of this DOS is similar to that of other proteins like myoglobin [10, 16]. The librational and torsional motions are embedded in lower frequency regions below 2000 cm^{-1} , and vibrational motions are located in higher frequency regions around 3000 cm^{-1} . There is a transparent region between 2000 cm^{-1} and 3000 cm^{-1} ; the peak due to the CD mode falls in this region near 2200 cm^{-1} . The VER of this CD mode is our target in this study. Note, furthermore, that the spectra in vacuum and in water are very similar: This indicates that water solvent might not affect the simulation results. This conjecture will be confirmed later.

3 Quantum correction factor approach

3.1 Fermi's golden rule

Our starting point is Fermi's golden rule formula for the population relaxation rate [13, 20]

$$\frac{1}{T_1} = \frac{2}{1 + e^{-\beta\hbar\omega_S}} \frac{1 - e^{-\beta\hbar\omega_S}}{\beta\hbar\omega_S} \int_0^\infty dt \cos(\omega_S t) \zeta(t) \quad (1)$$

where the force-force correlation function $\zeta(t)$ is defined as

$$\zeta(t) = \frac{\beta}{2m_S} \langle \mathcal{F}(t)\mathcal{F}(0) + \mathcal{F}(0)\mathcal{F}(t) \rangle_{\text{qm}}, \quad (2)$$

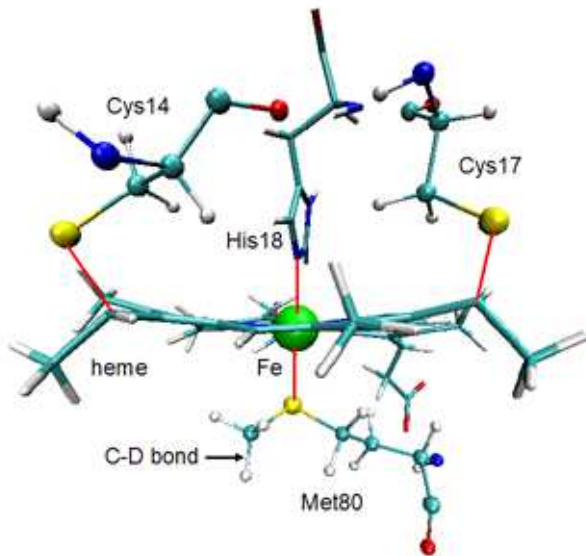


Figure 1: The structure of cytochrome c in the vicinity of the heme group, showing the thioether linkages and non-planar heme geometry.

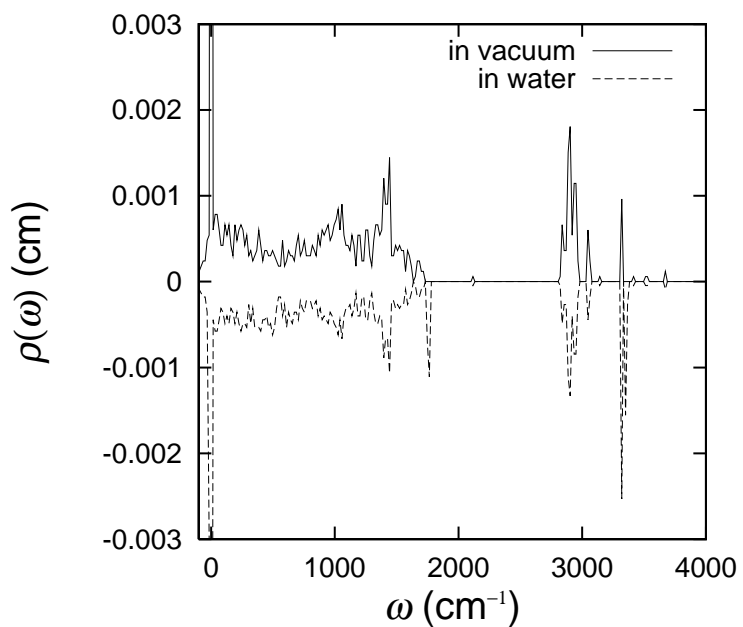


Figure 2: Density of states $\rho(\omega)$ for cytochrome c in vacuum (solid line) and in water (dashed line) at 300K.

(reduced) mass, ω_S is the system frequency, β is an inverse temperature, and the above bracket means a quantum mechanical average. Note that in the classical limit $\hbar \rightarrow 0$, the prefactor in front of the integral in Eq. (1) becomes unity, and the expression reduces to the well-known classical VER formula. The issue is that this limit does not represent well the VER for high frequency modes because of quantum effects (fluctuation), whereas it is difficult to calculate $\zeta(t)$ quantum mechanically.

3.2 Quantum correction factor

Bu and Straub [11] employed the quantum correction factor (QCF) strategy due to Skinner's group [12] and rewrote Eq. (1) as

$$\frac{1}{T_1^{\text{QCF}}} \simeq \frac{Q(\omega_S)}{\beta \hbar \omega_S} \int_0^\infty dt \cos(\omega_S t) \zeta_{\text{cl}}(t) = \frac{Q(\omega_S)}{\beta \hbar \omega_S} \tilde{\zeta}_{\text{cl}}(\omega_S) \quad (3)$$

where

$$\zeta_{\text{cl}}(t) = \frac{\beta}{m_S} \langle \mathcal{F}(t) \mathcal{F}(0) \rangle_{\text{cl}} \quad (4)$$

and the above bracket denotes a classical ensemble average. Note that the classical VER rate is defined as $1/T_1^{\text{cl}} \equiv \tilde{\zeta}_{\text{cl}}(\omega_S)$. Bu and Straub used the program CHARMM [21] to execute equilibrium simulations for cyt c *in water* at 300K [11]. For details of the simulations, see their original paper [11].

Here we report the similar calculations for cyt c *in vacuum* at 300K. In Fig. 3, the force autocorrelation function and its power spectrum are shown for four different trajectories. It turns out that the amount of the force fluctuation and the magnitude of the power spectrum for cyt c in vacuum is very similar to those computed for cyt c in water. Hence we conclude that the effects of water on the VER rate are negligible. With the CD bond frequency $\omega_S = 2133 \text{ cm}^{-1}$, we find $1/T_1^{\text{cl}} = \tilde{\zeta}_{\text{cl}}(\omega_S) \simeq 1 \text{ ps}^{-1}$, i.e. the classical VER time is about 1 ps.

As the CD stretching mode falls in the transparent region of the DOS (Fig. 2), a 1:1 Fermi resonance (linear resonance) is not the possible mechanism of VER. As such, the lowest order mechanism available for the VER of the CD mode should involve two phonons. We have employed the Skinner's QCF approach for two-phonon relaxation [12], that is

$$Q_{HH}(\omega_S) = Q_H(\omega_A)Q_H(\omega_S - \omega_A), \quad (5)$$

$$Q_{H-HS}(\omega_S) = Q_H(\omega_A) \sqrt{Q_H(\omega_S - \omega_A)} e^{\beta \hbar (\omega_S - \omega_A)/4}, \quad (6)$$

$$Q_H(\omega) = \frac{\beta \hbar \omega}{1 - e^{-\beta \hbar \omega}} \quad (7)$$

where ω_A is the frequency of an acceptor mode; Q_H, Q_{HH}, Q_{H-HS} are called a harmonic, harmonic-harmonic, harmonic-harmonic-Schofield QCF, respectively. To apply these QCFs to this situation, we need to know ω_A . We have found that the CD mode is strongly resonant with two lower frequency modes, 1655th (685.48 cm⁻¹) and 3823rd (1443.54 cm⁻¹) modes because $|\omega_S - \omega_{1655} - \omega_{3823}| = 0.03 \text{ cm}^{-1}$. Hence we might be able to choose $\omega_A = 1443.54 \text{ cm}^{-1}$ or 685.48 cm⁻¹.

In Fig. 4, we show ω_A dependence of the normalized QCF, i.e. $\tilde{Q} = Q/(\beta \hbar \omega_S) = T_1^{\text{cl}}/T_1^{\text{QCF}}$ at 300K and at 15K. If we choose $\omega_A = 1443.54 \text{ cm}^{-1}$ at 300K, $\tilde{Q} = 2.3$ for the harmonic-harmonic QCF and 2.8 for the harmonic-harmonic-Schofield QCF. Thus we have $T_1^{\text{QCF}} = T_1^{\text{cl}}/\tilde{Q} = 0.3 \sim 0.4 \text{ ps}$. It is interesting to note \tilde{Q} at 15K varies significantly depending on the QCF employed. We will discuss this feature later.

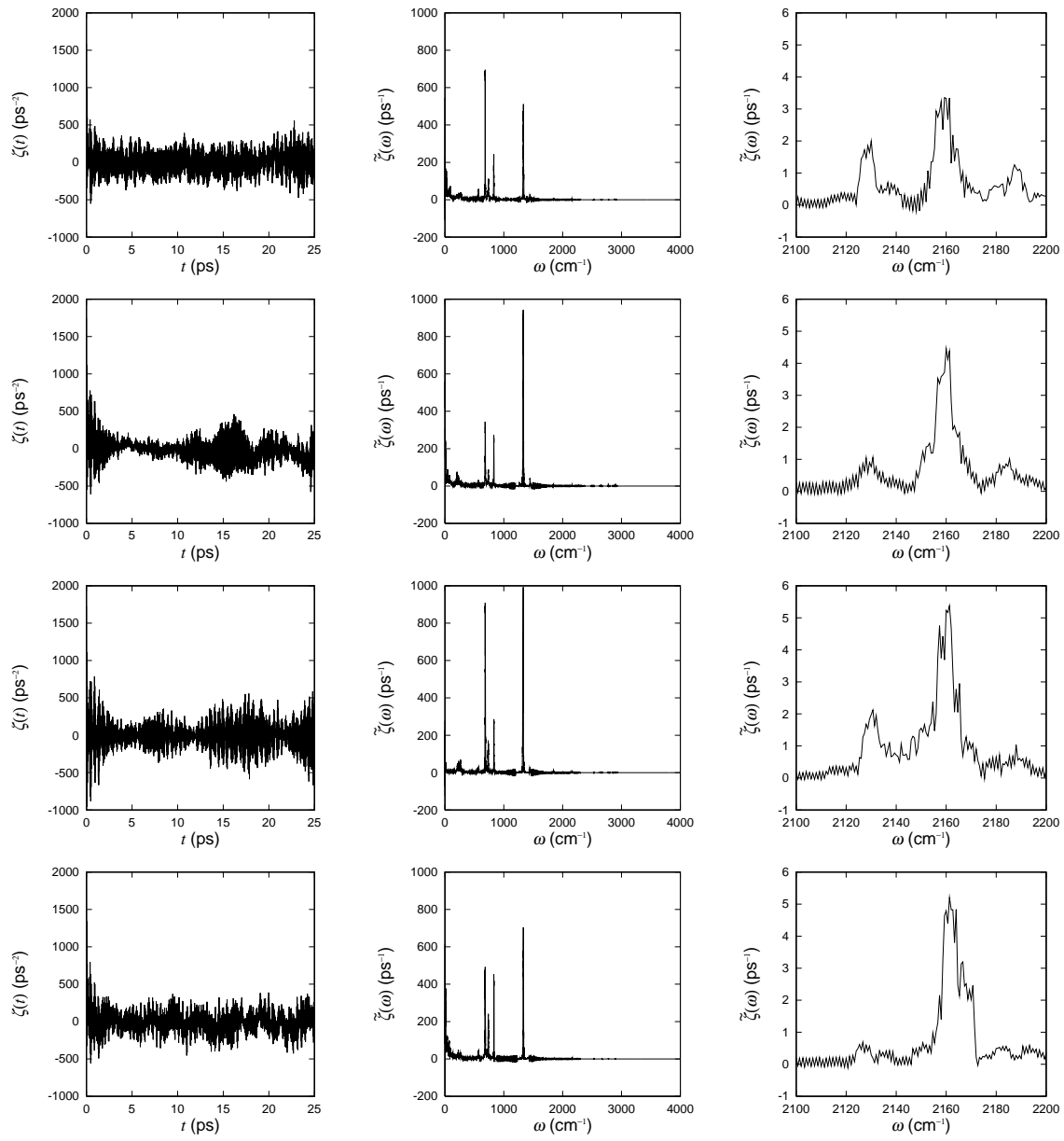


Figure 3: Left: Classical data for the force-force correlation function. Middle: Fourier spectra for the correlation function. Right: Magnification of the middle figures around the CD bond frequency. These data are taken from four different trajectories of the equilibrium simulation.

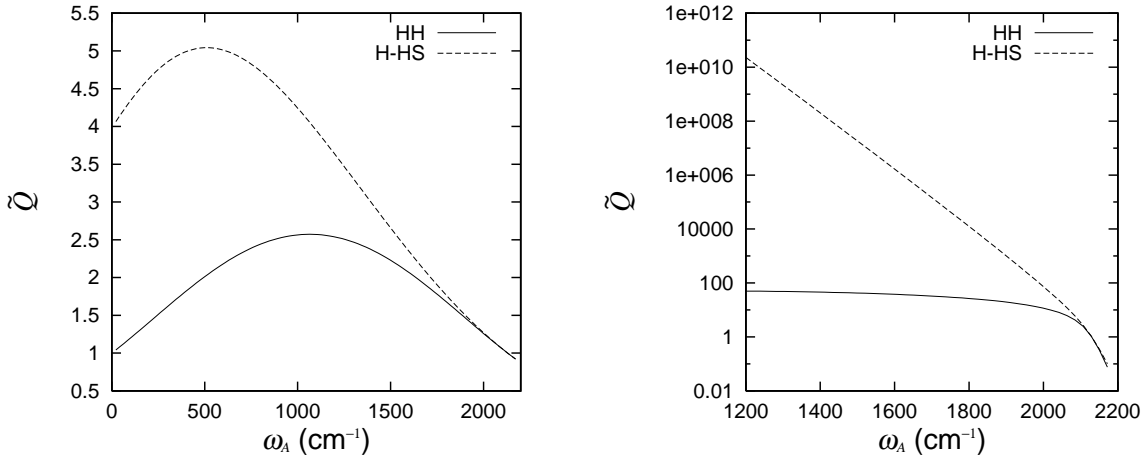


Figure 4: Normalized harmonic-harmonic (HH) and harmonic-harmonic-Schofield (H-HS) QCF at 300K (left) and at 15K (right).

3.3 Fluctuation of the CD mode frequency

We have discussed the fluctuation of the frequency for the CD bond [11]. In the equilibrium simulation, the instantaneous normal mode analysis has been employed for each instant of time to generate a time series $\omega_{CD}(t)$ for the CD bond frequency. From this time series, we can calculate the frequency autocorrelation function

$$C(t) = \overline{\delta\omega_{CD}(t)\delta\omega_{CD}(0)} = \frac{1}{T} \int_0^T d\tau \delta\omega_{CD}(t+\tau)\delta\omega_{CD}(\tau) \quad (8)$$

where the overline means a long time (T) average, and $\delta\omega_{CD}(t) = \omega_{CD}(t) - \overline{\omega_{CD}(t)}$. The correlation time is defined as

$$\tau_c = \frac{1}{(\Delta\omega)^2} \int_0^\infty C(t) dt \quad (9)$$

where $(\Delta\omega)^2 = C(0)$. From Fig. 5, we found $\Delta\omega \simeq 8 \text{ cm}^{-1}$ and $\tau_c \simeq 0.06 \text{ ps}$. Since $\Delta\omega\tau_c \ll 1$, according to Kubo's analysis [23], the lineshape should be homogeneously broadened, i.e., its shape is Lorentzian. This is also the case for cyt c in water [11]. We also confirmed that the potential barrier of the methyl group to rotate is significantly greater than the thermal energy (barrier height $\simeq 3 \text{ kcal/mol} >$ thermal energy $\simeq 0.6 \text{ kcal/mol}$) so that we do not expect inhomogeneity in the line shape.

These results support the validity of employing a normal mode type study of VER in cyt c as the structure of cyt c is rather rigid around the CD bond and the dynamics of the bond, on the scale of VER, should be well modeled by NMs. Of course, to describe VER among NMs, we must include nonlinear coupling terms. In the next section, we will discuss this reduced model approach for VER in cyt c.

4 Reduced model approach

4.1 Reduced model for a protein

The reduced model approach utilizes the normal mode picture of a protein, expanding the residual term perturbatively as [24]

$$\mathcal{H} = \mathcal{H}_S + \mathcal{H}_B + \mathcal{V}_3 + \mathcal{V}_4 + \dots, \quad (10)$$

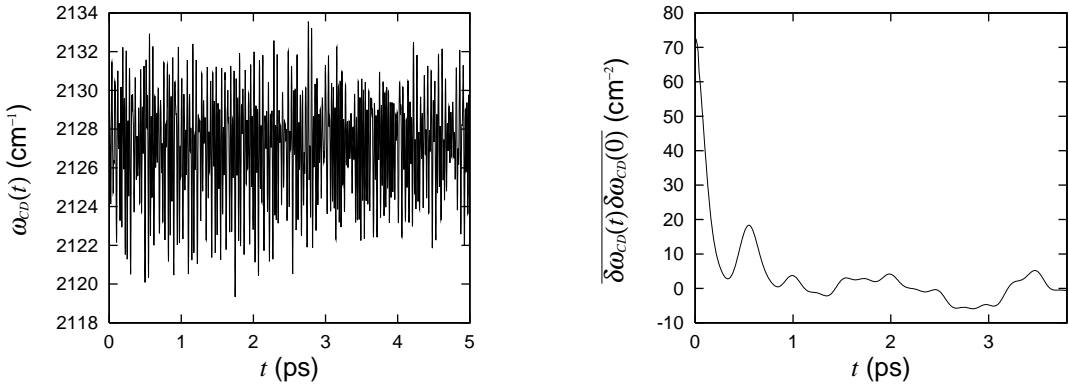


Figure 5: Left: The fluctuation of the CD bond frequency. Right: The frequency autocorrelation function. The data up to 20 ps were used to calculate the correlation function.

$$\mathcal{H}_S = \frac{p_S^2}{2} + \frac{\omega_S^2}{2} q_S^2, \quad (11)$$

$$\mathcal{H}_B = \sum_k \frac{p_k^2}{2} + \frac{\omega_k^2}{2} q_k^2, \quad (12)$$

$$\mathcal{V}_3 = \sum_{k,l,m} G_{klm} q_k q_l q_m, \quad (13)$$

$$\mathcal{V}_4 = \sum_{k,l,m,n} H_{klmn} q_k q_l q_m q_n. \quad (14)$$

Thus the force applied to the system mode is

$$\mathcal{F} = -\frac{\partial \mathcal{V}}{\partial q_S} = -3 \sum_{k,l} G_{S,k,l} q_k q_l - 4 \sum_{k,l,m} H_{S,k,l,m} q_k q_l q_m + \dots \quad (15)$$

where we have used the permutation symmetry of G_{klm} and H_{klmn} . If it is enough to include the lowest order terms proportional to G_{klm} , substituting them into Fermi's golden rule Eq. (1), we can derive an approximate VER rate as [13]

$$\frac{1}{T_1} \simeq \frac{1}{m_S \hbar \omega_S} \frac{1 - e^{-\beta \hbar \omega_S}}{1 + e^{-\beta \hbar \omega_S}} \sum_{k,l} \left[\frac{\gamma \zeta_{k,l}^{(+)}}{\gamma^2 + (\omega_k + \omega_l - \omega_S)^2} + \frac{\gamma \zeta_{k,l}^{(+)}}{\gamma^2 + (\omega_k + \omega_l + \omega_S)^2} \right. \\ \left. + \frac{\gamma \zeta_{k,l}^{(-)}}{\gamma^2 + (\omega_k - \omega_l - \omega_S)^2} + \frac{\gamma \zeta_{k,l}^{(-)}}{\gamma^2 + (\omega_k - \omega_l + \omega_S)^2} \right] \quad (16)$$

where we have included a width parameter γ to broaden a delta function, and defined the following

$$\zeta_{k,l}^{(+)} = \frac{\hbar^2}{2} \frac{(A_{k,l}^{(2)})^2}{\omega_k \omega_l} (1 + n_k + n_l + 2n_k n_l), \quad (17)$$

$$\zeta_{k,l}^{(-)} = \frac{\hbar^2}{2} \frac{(A_{k,l}^{(2)})^2}{\omega_k \omega_l} (n_k + n_l + 2n_k n_l), \quad (18)$$

$$A_{k,l}^{(2)} = -3G_{S,k,l}, \quad (19)$$

$$n_k = 1/(e^{\beta \hbar \omega_k} - 1). \quad (20)$$

There exists another well known formula to describe the VER rate, the Maradudin-Fein (MF) formula [25, 14],

$$W = W_{\text{decay}} + W_{\text{coll}}, \quad (21)$$

$$W_{\text{decay}} = \frac{\hbar}{2m_S\omega_S} \sum_{k,l} \frac{(A_{k,l}^{(2)})^2}{\omega_k\omega_l} (1 + n_k + n_l) \frac{\gamma}{\gamma^2 + (\omega_S - \omega_k - \omega_l)^2}, \quad (22)$$

$$W_{\text{coll}} = \frac{\hbar}{m_S\omega_S} \sum_{k,l} \frac{(A_{k,l}^{(2)})^2}{\omega_k\omega_l} (n_k - n_l) \frac{\gamma}{\gamma^2 + (\omega_S + \omega_k - \omega_l)^2} \quad (23)$$

with a width parameter γ . Note that Eq. (16) and Eq. (21) are equivalent in the limit of $\gamma \rightarrow 0$ as shown by Fayer's group [26]. However, they disagree with a finite width parameter such as $\gamma \sim 100 \text{ cm}^{-1}$. In this chapter, we use the MF formula and consider its classical limit ($\hbar \rightarrow 0$) defined as

$$W_{\text{decay}}^{\text{cl}} = \frac{1}{2m_S\beta\omega_S} \sum_{k,l} \frac{(A_{k,l}^{(2)})^2}{\omega_k\omega_l} \left(\frac{1}{\omega_k} + \frac{1}{\omega_l} \right) \frac{\gamma}{\gamma^2 + (\omega_S - \omega_k - \omega_l)^2}, \quad (24)$$

$$W_{\text{coll}}^{\text{cl}} = \frac{1}{m_S\beta\omega_S} \sum_{k,l} \frac{(A_{k,l}^{(2)})^2}{\omega_k\omega_l} \left(\frac{1}{\omega_k} - \frac{1}{\omega_l} \right) \frac{\gamma}{\gamma^2 + (\omega_S + \omega_k - \omega_l)^2}. \quad (25)$$

We note some properties of the formula: $W_{\text{decay}} \geq W_{\text{decay}}^{\text{cl}}$ and $W_{\text{coll}} \leq W_{\text{coll}}^{\text{cl}}$ which is derived from

$$\frac{1/(e^x - 1) + 1/(e^y - 1)}{1/x + 1/y} \geq 1, \quad (26)$$

$$\frac{1/(e^x - 1) - 1/(e^y - 1)}{1/x - 1/y} \leq 1 \quad (27)$$

for $x, y > 0$. We can define an effective QCF as

$$Q_{\text{eff}} = \frac{W}{W^{\text{cl}}} = \frac{W_{\text{decay}} + W_{\text{coll}}}{W_{\text{decay}}^{\text{cl}} + W_{\text{coll}}^{\text{cl}}}. \quad (28)$$

This should be compared with the normalized QCFs [$\tilde{Q} = Q(\omega_S)/(\beta\hbar\omega_S)$] found in the literature.

4.3 Third order coupling elements

To calculate the third order coupling elements, we use the formula

$$A_{mn}^{(2)} = -\frac{1}{2} \frac{\partial^3 V}{\partial q_S \partial q_m \partial q_n} \simeq -\frac{1}{2} \sum_{ij} U_{im} U_{jn} \frac{K_{ij}(\Delta q_S) - K_{ij}(-\Delta q_S)}{2\Delta q_S} \quad (29)$$

where U_{ik} is an orthogonal matrix that diagonalizes the (mass-weighted) hessian matrix at the mechanically stable structure K_{ij} , and $K_{ij}(\pm\Delta q_S)$ is a hessian matrix calculated at a shifted structure along the direction of a selected mode with a shift $\pm\Delta q_S$. See [13] for the details.

We show the width parameter γ dependence of the VER rate in Fig. 6.¹ We consider other lower frequency modes ($\omega_{3330} = 1330.9 \text{ cm}^{-1}$, $\omega_{1996} = 829.9 \text{ cm}^{-1}$, $\omega_{1655} = 685.5 \text{ cm}^{-1}$) as well as the CD mode ($\omega_{CD} = 2129.1 \text{ cm}^{-1}$) for comparison. From the former analysis of the frequency autocorrelation function Eq. (8), we might be able to take $\gamma \simeq \Delta\omega \sim 3 \text{ cm}^{-1}$ for the CD mode, and we have $T_1 \simeq 0.2 \text{ ps}$, which agrees with the previous result with QCFs: $T_1^{\text{QCF}} = 0.3 \sim 0.4 \text{ ps}$. We also see that the lower frequency modes have longer VER time, a few ps, which agrees with the calculations by Leitner's group employing the MF formula [15]. The main contribution to the VER rate at $\gamma = 3 \text{ cm}^{-1}$ comes from 1655th (685.5 cm^{-1}) and 3823rd (1443.5 cm^{-1}) modes ($\sim 20\%$). Interestingly, we can conceive a peak around $\gamma = 0.03 \text{ cm}^{-1}$. Given this width parameter, the contribution from the two modes is more than 90%. In any case, we can say that 1655th and 3823rd modes are resonant with the CD mode because they satisfy the resonant condition ($|\omega_{1655} + \omega_{3823} - \omega_{CD}| \simeq 0.03 \text{ cm}^{-1}$) and the coupling elements between them is relatively large ($|A_{1655,3823}^{(2)}| \simeq 5.1 \text{ kcal/mol/}\text{\AA}^3$).

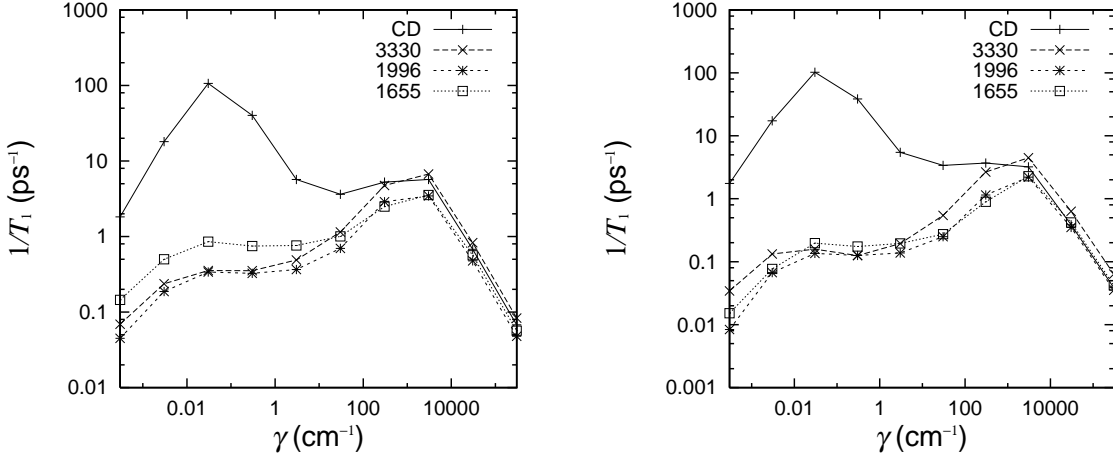


Figure 6: VER rates for the CD mode ($\omega_{CD} = 2129.1 \text{ cm}^{-1}$) and the other lower frequency modes ($\omega_{3330} = 1330.9 \text{ cm}^{-1}$, $\omega_{1996} = 829.9 \text{ cm}^{-1}$, $\omega_{1655} = 685.5 \text{ cm}^{-1}$) as a function of γ at 300K (left) and at 15K (right).

In the left of Fig. 7, we show the effective QCF calculated from Eq. (28) at 300K, which is $Q_{\text{eff}} \simeq 2.3$ for the CD mode with $\gamma = 3 \text{ cm}^{-1}$. This value better agrees with the (normalized) harmonic-harmonic QCF [Eq. (5)], compared to the harmonic-harmonic-Schofield QCF [Eq. (6)]. The Q_{eff} for the other modes are more or less unity, which indicates that these modes behave classically at 300K.² In contrast, as is shown in the right of Fig. 7, Q_{eff} at 15K is very large ($Q_{\text{eff}} \simeq 40$), which implies that the classical VER rate becomes small because it is proportional to the temperature (see also Fig. 8). A similar trend is found in the right of Fig. 4, where the harmonic-harmonic QCF ($\tilde{Q} \simeq 40$) is comparable to Q_{eff} . On the other hand, the harmonic-harmonic-Schofield QCF gives an exponentially large value of \tilde{Q} , showing strong deviations from Q_{eff} . We should bear in mind that different QCFs lead to significantly different conclusions at low temperatures.

¹Note two limiting cases of γ dependence: $1/T_1 \propto \gamma$ when γ is very small, and $1/T_1 \propto 1/\gamma$ when γ is very large. This is easily recognized from the Lorentzian form.

²We notice an interesting behavior for 1655th mode, i.e. Q_{eff} becomes very much smaller than unity at $\gamma \simeq 0.03 \text{ cm}^{-1}$. In this case, we observe that $W_{\text{coll}} \gg W_{\text{decay}}$ because of the resonance: $\omega_{1655} + \omega_{3823} - \omega_{CD} \simeq 0$ (actually 0.03 cm^{-1}). In such a case, Q_{eff} becomes less than unity because $W_{\text{coll}} \leq W_{\text{coll}}^{\text{cl}}$.

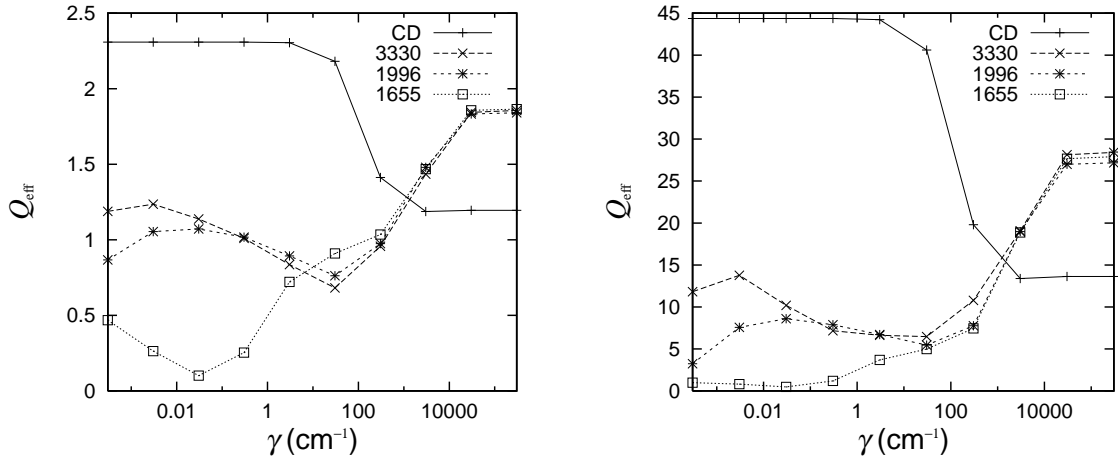


Figure 7: Effective QCF for the CD mode ($\omega_{CD} = 2129.1 \text{ cm}^{-1}$) and the other lower frequency modes ($\omega_{3330} = 1330.9 \text{ cm}^{-1}$, $\omega_{1996} = 829.9 \text{ cm}^{-1}$, $\omega_{1655} = 685.5 \text{ cm}^{-1}$) as a function of γ at 300K (left). and at 15K (right).

4.5 Temperature dependence

In Fig. 8, we show the temperature dependence of the quantum and classical VER rate calculated by the MF formula and the classical limit of the MF formula. At high temperatures ($\sim 1000\text{K}$), the quantum VER rate agrees with the classical one, but they deviate at low temperatures. The former becomes constant due to the remaining quantum fluctuation (zero point energy) whereas the latter decreases as $\propto (T)$. The “cross over temperature” where the VER behaves classically is smaller for the lower frequency modes compared to that of the CD mode.

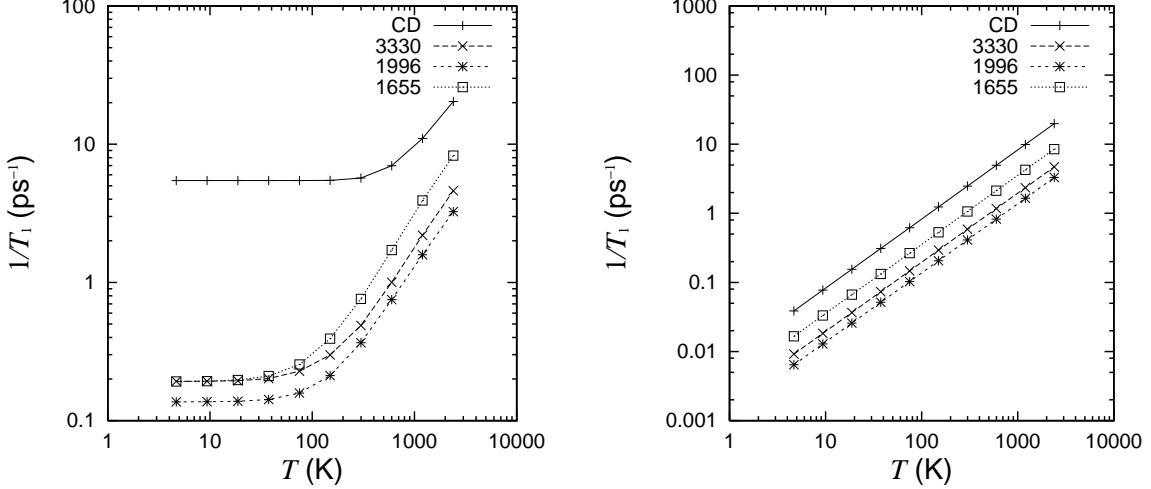


Figure 8: Quantum (left) and classical (right) VER rates for the CD mode ($\omega_{CD} = 2129.1 \text{ cm}^{-1}$) and the other lower frequency modes ($\omega_{3330} = 1330.9 \text{ cm}^{-1}$, $\omega_{1996} = 829.9 \text{ cm}^{-1}$, $\omega_{1655} = 685.5 \text{ cm}^{-1}$) as a function of temperature with $\gamma = 3 \text{ cm}^{-1}$.

5.1 Comparison with experiment

Here we compare our results with the experiment by Romeberg's group [19]. They measured the shifts and widths of the spectra for different forms of cyt c; the widths of the spectra (FWHM) were found to be $\Delta\omega_{\text{FWHM}} \simeq 6.0 \sim 13.0 \text{ cm}^{-1}$. From the discussions of Sec. 3.3, we can theoretically neglect inhomogeneous effects, and estimate the VER rate simply as

$$T_1 \sim 5.3/\Delta\omega_{\text{FWHM}} (\text{ps}) \quad (30)$$

which corresponds to $T_1 \simeq 0.4 \sim 0.9 \text{ ps}$. This estimate is similar to the QCF prediction using Eq. (3) ($0.3 \sim 0.4 \text{ ps}$) and the reduced model approach using Eq. (16) or (21) ($0.2 \sim 0.3 \text{ ps}$). We note that this value should be compared to the VER time of the C-H stretch in N-methylacetamide-D [$\text{CH}_3(\text{CO})\text{ND}(\text{CH}_3)$] [22], which is also sub ps. Further experimental studies, e.g. on temperature dependence of absorption spectra or on time-resolved spectroscopy, will clarify which methodology is more applicable.

Romesberg's group studied Met80-3D (methionine with three deuteriums) while we have examined Met80-1D (methionine with one deuterium). In the case of Met80-3D, apparently, there appear three peaks in the transparent region. Hence it will be possible to consider the VER of three such modes to compare with their experiments.

5.2 Validity of Fermi's golden rule

We next discuss the validity of our approaches. Since our starting point is the perturbative Fermi's golden rule, our two approaches should have a limited range of validity. Naively speaking, the force applied on the CD mode should be small enough, but how small it should be?

We follow Kubo's derivation of a quantum master equation using the projection operator technique [23]. He derived an equation for the evolution of the system density operator $\sigma(t)$

$$\begin{aligned} \frac{\partial}{\partial t}\sigma(t) = & -\frac{1}{\hbar^2} \int_{-\infty}^t d\tau [q(t)q(\tau)\sigma(\tau)\Phi(t-\tau) - q(t)\sigma(\tau)q(\tau)\Phi(-t+\tau) \\ & + \sigma(\tau)q(\tau)q(t)\Phi(-t+\tau) - q(\tau)\sigma(\tau)q(t)\Phi(t-\tau)]. \end{aligned} \quad (31)$$

The interaction Hamiltonian is assumed to be $\mathcal{H}_{\text{int}} = -q\mathcal{F}$, as in our case, i.e. q is the system coordinate and \mathcal{F} mainly contains the bath coordinates. We have defined the force autocorrelation function $\Phi(t) = \text{Tr}_B\{\rho_B\mathcal{F}(t)\mathcal{F}(0)\} = \langle\mathcal{F}(t)\mathcal{F}(0)\rangle$. Note that Eq. (31) is just a von Neumann equation using the projection operator technique, and it is not a master equation yet.

If $\Phi(t)$ decays fast, we can replace $\sigma(\tau)$ in the integral with $\sigma(t)$, and the dynamics becomes an approximate Markovian dynamics. If this approximation is valid, Fermi's golden rule describes the relaxation dynamics of $\sigma(t)$ [23]. Hence the validity of the golden rule relies on the validity of the Markov approximation.

From Eq. (31), the relaxation rate of $\sigma(t)$ can be estimated as

$$1/\tau_r \sim (\langle q^2 \rangle \mathcal{F}^2 / \hbar^2) \tau_c \quad (32)$$

where we have assumed

$$\Phi(t) \simeq \mathcal{F}^2 e^{-|t|/\tau_c}. \quad (33)$$

The Markov approximation [$\sigma(\tau) \simeq \sigma(t)$] holds for

$$\tau_r \gg \tau_c. \quad (34)$$

$$\epsilon \equiv \langle q^2 \rangle \mathcal{F}^2 \tau_c^2 / \hbar^2 \ll 1. \quad (35)$$

In our case as well as the case of HOD in D₂O, the ratio is “just” small enough (see Table 1). Applying Fermi’s golden rule to these situations should be regarded as a reasonable estimate of the VER rate. As an alternative approach that may avoid this underlying Markov approximation, one might employ a nonequilibrium MD [27] though such a method is quasi-classical in nature.

Table 1: The parameters in Eq. (35) for various molecules in AKMA units (unit length = 1 Å, unit time = 0.04888 ps, unit energy = 1 kcal/mol). The data for HOD in D₂O, CN[−] in water, and CO in Mb are taken from [28], [29], and [10], respectively.

	$\langle q^2 \rangle$	\mathcal{F}^2	τ_c	ϵ
CD in cyt c	0.01	5.0	1.0	0.5
HOD in D ₂ O	0.01	5.0	1.0	0.5
CN [−] in water	0.002	1.0	0.5	0.01
CO in Mb	0.002	1.0	1.0	0.02

5.3 Higher order coupling terms

Up to now, we have only included the third order coupling terms to describe the VER of the CD mode. However, we must be concerned with the relative contribution of higher order mechanism, e.g. the contribution due to the fourth order coupling terms in Eq. (14). This is a very difficult question. As there are many terms ($\sim 10^9$) included, we cannot directly calculate all of them for cyt c. We have found that it is not sufficient to include only the third order coupling terms to reproduce the fluctuation of the force on the CD bond. However, this does not necessarily mean that the VER rate calculated from the third order coupling terms is inadequate.

The main contribution from the fourth order coupling terms to the VER rate and the force fluctuation are written as

$$\Delta \left(\frac{1}{T_1} \right) \sim \sum_{k,l,m} \frac{|H_{S,k,l,m}|^2}{\omega_k \omega_l \omega_m} \delta(\omega_S - \omega_k - \omega_l - \omega_m), \quad (36)$$

and

$$\Delta \langle \delta \mathcal{F}^2 \rangle \sim \sum_{k,l,m} \frac{|H_{S,k,l,m}|^2}{\omega_k \omega_l \omega_m}, \quad (37)$$

respectively. Hence, even if $\Delta \langle \delta \mathcal{F}^2 \rangle$ becomes large, $\Delta (1/T_1)$ is not necessarily large because of the resonance condition: $\omega_S - \omega_k - \omega_l - \omega_m \simeq 0$. To circumvent this situation, we might need to employ a nonequilibrium MD method [27]. By comparing the nonequilibrium dynamics for the whole system and the reduced system up to the third order coupling elements, we might determine the relative importance of the fourth or higher order coupling terms.

6 Summary

In this chapter, we have examined VER in a protein from the QCF approach and the reduced model approach, and compared the results. For the CD mode in cyt c (in vacuum) at room

to an estimate based on an experiment by Romesberg's group. A weakness of the QCF approach is that we don't know which QCF to choose a priori and this causes a significant difference at lower temperatures. On the other hand, a weakness of the reduced model approach is that the method neglects the higher order coupling elements more than the third, which cannot be justified a priori. Hence we need to proceed this kind of comparative study to correctly describe the VER in proteins. As for the other methods used to examine VER in molecules, we name the nonequilibrium MD method [27], the time-dependent Hartree method [30], and the semiclassical methods [31, 32]. Finally, to compare with experiments, we need to calculate spectroscopic observables such as absorption spectra or 2D-IR signals [33, 34]. These observables will provide us with a more detailed view of VER, the nonlinear coupling elements, and the dynamics of the protein.

7 Acknowledgement

We thank Prof. S. Takada, Prof. T. Komatsuzaki, Prof. Y. Mizutani, Prof. K. Tominaga, Prof. F. Romesberg, Prof. J.L. Skinner, Prof. D.M. Leitner, Prof. I. Ohmine, Prof. S. Saito, Prof. R. Akiyama, Prof. K. Takatsuka, Dr. H. Ushiyama, Dr. T. Miyadera, Dr. S. Fuchigami, Dr. T. Yamashita, Dr. Y. Sugita, Dr. M. Ceremeens, Dr. J. Zimmerman, and Dr. P.H. Nguyen for helpful comments and discussions, and Prof. S. Mukamel and Prof. Y. Tanimura for informing the references related to nonlinear spectroscopy.

References

- [1] N. Go, T. Noguchi, and T. Nishikawa, "Dynamics of a small protein in terms of low-frequency vibrational modes," *Proc. Natl. Acad. Sci. U.S.A* **80**, 3696 (1983); B. Brooks and M. Karplus, "Harmonic dynamics of proteins: Normal modes and fluctuations in bovine pancreatic trypsin inhibitor," *ibid.* **80**, 6571 (1983).
- [2] J. A. McCammon, B.R. Gelin, M. Karplus, and P.G. Wolynes, "The Hinge-Bending Mode in Lysozyme," *Nature* **262**, 325 (1976).
- [3] A. Kidera and N. Go, "Refinement of protein dynamic structure: Normal mode refinement," *Proc. Natl. Acad. Sci. U.S.A* **87**, 3718 (1990).
- [4] D. Ming, Y. Kong, M.A. Lambert, Z. Huang, and J. Ma, "How to describe protein motion without amino acid sequence and atomic coordinates," *Proc. Natl. Acad. Sci. U.S.A* **99**, 8620 (2002).
- [5] G. Li and Q. Cui, "A coarse-grained normal mode approach for macromolecules: An efficient implementation and application to Ca^{2+} -ATPase," *Biophys. J.* **83**, 2457 (2002).
- [6] F. Tama, M. Valle, J. Frank, and C.L. Brooks III, "Dynamic reorganization of the functionally active ribosome explored by normal mode analysis and cryo-electron microscopy," *Proc. Natl. Acad. Sci. U.S.A* **100**, 9319 (2003).
- [7] Y. Mizutani and T. Kitagawa, "Direct observation of cooling of heme upon photodissociation of carbonmonoxy myoglobin," *Science* **278**, 443 (1997); "Ultrafast structural relaxation of myoglobin following photodissociation of carbon monoxide probed by time-resolved resonance Raman spectroscopy," *J. Phys. Chem. B* **105**, 10992 (2001); M.D. Fayer, "Fast protein dynamics probed with infrared vibrational echo experiments," *Ann. Rev. Phys. Chem.* **52**, 315 (2001); X. Ye, A. Demidov, and P.M. Champion, "Measurements of the photodissociation quantum yields of MbNO and MbO_2 and the vibrational

Rosca, A.T.N. Kumar, D. Ionascu, X. Ye, A.A. Demidov, T. Sjodin, D. Wharton, D. Barrick, S.G. Sligar, T. Yonetani, and P.M. Champion, "Investigations of Anharmonic Low-Frequency Oscillations in Heme Proteins," *J. Phys. Chem. A* **106**, 3540 (2002).

[8] B.J. Berne, M. Borkovec, and J.E. Straub, "Classical and Modern Methods in Reaction Rate Theory," *J. Phys. Chem.* **92**, 3711 (1988); J.I. Steinfeld, J.E. Francisco, and W.L. Hase, *Chemical Kinetics and Dynamics*, Prentice-Hall (1989); A. Stuchebrukhov, S. Ionov, and V. Letokhov, "IR spectra of highly vibrationally excited large polyatomic molecules and intramolecular relaxation," *J. Phys. Chem.* **93**, 5357 (1989); T. Uzer, "Theories of intramolecular vibrational energy transfer," *Phys. Rep.* **199**, 73 (1991).

[9] D.E. Logan and P.G. Wolynes, "Quantum localization and energy flow in many-dimensional Fermi resonant systems," *J. Chem. Phys.* **93**, 4994 (1990); S.A. Schofield and P.G. Wolynes, "A scaling perspective on quantum energy flow in molecules," *J. Chem. Phys.* **98**, 1123 (1993); S.A. Schofield, P.G. Wolynes, and R.E. Wyatt, "Computational study of many-dimensional quantum energy flow: From action diffusion to localization," *Phys. Rev. Lett.* **74**, 3720 (1995); S.A. Schofield and P.G. Wolynes, "Rate theory and quantum energy flow in molecules: Modeling the effects of anisotropic diffusion and dephasing," *J. Phys. Chem.* **99**, 2753 (1995); D.M. Leitner and P.G. Wolynes, "Vibrational mixing and energy flow in polyatomics: Quantitative prediction using local random matrix theory," *J. Phys. Chem. A* **101**, 541 (1997).

[10] D.E. Sagnella and J.E. Straub, "A study of vibrational relaxation of B-state carbon monoxide in the heme pocket of photolyzed carboxymyoglobin," *Biophys. J.* **77**, 70 (1999).

[11] L. Bu and J.E. Straub, "Vibrational frequency shifts and relaxation rates for a selected vibrational mode in cytochrome c," *Biophys. J.* **85**, 1429 (2003).

[12] J.L. Skinner and K. Park, "Calculating vibrational energy relaxation rates from classical molecular dynamics simulations: quantum correction factors for processes involving vibration-vibration energy transfer," *J. Phys. Chem. B* **105**, 6716 (2001).

[13] H. Fujisaki, L. Bu, and J.E. Straub, *Adv. Chem. Phys.* (in press); e-print q-bio.BM/040319.

[14] D.M. Leitner, "Vibrational energy transfer in helices," *Phys. Rev. Lett.* **87**, 188102 (2001); X. Yu and D.M. Leitner, "Vibrational energy transfer and heat conduction in a protein," *J. Phys. Chem. B* **107**, 1698 (2003).

[15] D.M. Leitner, private communication.

[16] K. Moritsugu, O. Miyashita, and A. Kidera, "Vibrational Energy Transfer in a Protein Molecule," *Phys. Rev. Lett.* **85**, 3970 (2000); "Temperature Dependence of Vibrational Energy Transfer in a Protein Molecule," *J. Phys. Chem. B* **107**, 3309 (2003).

[17] David Keilin, *The History of Cell Respiration and Cytochrome*, Cambridge University Press, Cambridge (1966); Richard E. Dickerson, "Cytochrome c and the evolution of energy metabolism," *Sci. Am.* **242**, 136 (1980); G.W. Pettigrew and G.R. Moore, *Cytochromes c: Evolutionary, Structural, and Physiochemical Aspects*, Springer-Verlag, Berlin (1990).

[18] S.H. Northrup, M.P. Pear, J.A. McCammon, and M. Karplus, "Molecular dynamics of ferrocytocrome c," *Nature* **286**, 304 (1980); C.F. Wong, C. Zheng, J. Shen, J.A. McCammon, and P.G. Wolynes, "Cytochrome c: A molecular proving ground for computer simulations," *J. Phys. Chem.* **97**, 3100 (1993); A.E. García and G. Hummer, "Conformational dynamics of cytochrome c: Correlation to hydrogen exchange," *Proteins: Struct.*

foldings: Atomically detailed simulations," *ibid.* **51**, 245 (2003); X. Yu and D.M. Leitner, "Anomalous diffusion of vibrational energy in proteins," *J. Chem. Phys.* **119**, 12673 (2003).

[19] J.K. Chin, R. Jimenez, and F. Romesberg, "Direct observation of protein vibrations by selective incorporation of spectroscopically observable carbon-deuterium bonds in cytochrome c," *J. Am. Chem. Soc.* **123**, 2426 (2001); "Protein dynamics and cytochrome c: Correlation between ligand vibrations and redox activity," *ibid.* **124**, 1846 (2002).

[20] J.S. Bader and B.J. Berne, "Quantum and classical relaxation rates from classical simulations," *J. Chem. Phys.* **100**, 8359 (1994).

[21] B.R. Brooks, R.E. Bruccoleri, B.D. Olafson, D.J. States, S. Swaminathan, and M. Karplus, "CHARMM: A Program for Macromolecular Energy, Minimization, and Dynamics Calculations," *J. Comp. Chem.* **4**, 187 (1983); A.D. MacKerell, Jr., B. Brooks, C.L. Brooks III, L. Nilsson, B. Roux, Y. Won, and M. Karplus, "CHARMM: The Energy Function and Its Parameterization with an Overview of the Program," in *The Encyclopedia of Computational Chemistry*, **1**, 271, P.v.R. Schleyer et al., editors, John Wiley & Sons: Chichester (1998).

[22] P. Hamm, M. Lim, and R.M. Hochstrasser, "Structure of the amide I band of peptides measured by femtosecond nonlinear-infrared spectroscopy," *J. Phys. Chem. B* **102**, 6123 (1998).

[23] R. Kubo, M. Toda, and N. Hashitsume, *Statistical Physics II, Nonequilibrium Statistical Mechanics*, Springer-Verlag, Berlin (1991).

[24] M. Shiga and S. Okazaki, "An influence functional theory of multiphonon processes in molecular vibrational energy relaxation," *J. Chem. Phys.* **109**, 3542 (1998); "Molecular dynamics study of vibrational energy relaxation of CN⁻ in H₂O and D₂O solutions: An application of path integral influence functional theory to multiphonon processes," *ibid.* **111**, 5390 (1999); T. Mikami, M. Shiga and S. Okazaki, "Quantum effect of solvent on molecular vibrational energy relaxation of solute based upon path integral influence functional theory," *ibid.* **115**, 9797 (2001).

[25] A.A. Maradudin and A.E. Fein, "Scattering of neutrons by an anharmonic crystal," *Phys. Rev.* **128**, 2589 (1962).

[26] V.M. Kenkre, A. Tokmakoff, and M.D. Fayer, "Theory of vibrational relaxation of polyatomic molecules in liquids," *J. Chem. Phys.* **101**, 10618 (1994).

[27] P.H. Nguyen and G. Stock, "Nonequilibrium molecular-dynamics study of the vibrational energy relaxation of peptides in water," *J. Chem. Phys.* **119**, 11350 (2003).

[28] R. Rey and J.T. Hynes, "Vibrational energy relaxation of HOD in liquid D₂O," *J. Chem. Phys.* **104**, 2356 (1996).

[29] R. Rey and J.T. Hynes, "Vibrational phase and energy relaxation of CN⁻ in water," *J. Chem. Phys.* **108**, 142 (1998).

[30] R.B. Gerber, V. Buch, and M.A. Ratner, "Time-dependent self-consistent field approximation for intramolecular energy transfer. I. Formulation and application to dissociation of van der Waals molecules," *J. Chem. Phys.* **77**, 3022 (1982); A. Roitberg, R.B. Gerber, R. Elber, and M.A. Ratner, "Anharmonic Wave Functions of Proteins: Quantum Self-Consistent Field Calculations of BPTI," *Science*, **268**, 1319 (1995); S.K. Gregurick,

water complexes: Anharmonic coupled-mode calculations," *J. Phys. Chem. B* **101**, 8595 (1997); Z. Bihary, R.B. Gerber, and V.A. Apkarian, "Vibrational self-consistent field approach to anharmonic spectroscopy of molecules in solids: Application to iodine in argon matrix," *J. Chem. Phys.* **115**, 2695 (2001). For a review of the VSCF methods, see P. Jungwirth and R.B. Gerber, "Quantum Molecular Dynamics of Ultrafast Processes in Large Polyatomic Systems," *Chem. Rev.* **99**, 1583 (1999).

- [31] Q. Shi and E. Geva, "Semiclassical theory of vibrational energy relaxation in the condensed phase," *J. Phys. Chem. A* **107**, 9059 (2003); "Vibrational energy relaxation in liquid oxygen from a semiclassical molecular dynamics simulation," *ibid.* **107**, 9070 (2003); "On the calculation of vibrational energy relaxation rate constants from centroid molecular dynamics simulations," *J. Chem. Phys.* **119**, 9030 (2003).
- [32] H. Kim and P.J. Rossky, "Evaluation of quantum correlation functions from classical data," *J. Phys. Chem. B* **106**, 8240 (2002); J.A. Poulsen, G. Nyman, and P.J. Rossky, "Practical evaluation of condensed phase quantum correlation functions: A Feynman-Kleinert variational linearized path integral method," *J. Chem. Phys.* **119**, 12179 (2003).
- [33] S. Mukamel and D. Abramavicius, "Many-body approaches for simulating coherent nonlinear spectroscopies of electronic and vibrational excitons," *Chem. Rev.* **104**, 2073 (2004).
- [34] T. Kato and Y. Tanimura, "Multi-dimensional vibrational spectroscopy measured from different phase-matching conditions," *Chem. Phys. Lett.* **341**, 329 (2001); K. Okumura and Y. Tanimura, "Sensitivity of two-dimensional fifth-order Raman response to the mechanism of vibrational mode-mode coupling in liquid molecules," *Chem. Phys. Lett.* **278**, 175 (1997).

